8-27-2001

Airglow Variations Associated with Nonideal Ducting of Gravity Waves in the Lower Thermosphere Region

Michael P. Hickey Ph.D.
Embry-Riddle Aeronautical University, hicke0b5@erau.edu

Scholarly Commons Citation

Hickey, M. P. (2001), Airglow variations associated with nonideal ducting of gravity waves in the lower thermosphere region, J. Geophys. Res., 106(D16), 17907–17917, doi: https://doi.org/10.1029/2001JD900182

JOURNAL OF GEOPHYSICAL RESEARCH, VOL. 106, NO. D16, PAGES 17,907–17,917, AUGUST 27, 2001

Airglow variations associated with nonideal ducting of gravity waves in the lower thermosphere region

Michael P. Hickey

Department of Physics and Astronomy, Clemson University, Clemson, South Carolina

Abstract. A numerical full-wave model is used to study the response of the O_2 atmospheric airglow to ducted gravity waves in the mesopause region. For an isothermal, quasi-adiabatic, and motionless background atmosphere the calculated phase differences between airglow brightness fluctuations and fluctuations of temperatures derived from the airglow, as given by Krassovsky's ratio, are in good agreement with the predictions of published theory. Significant departures from the predictions of the basic theory are obtained when we consider ducting in the presence of the eddy and molecular diffusion of heat and momentum in a nonisothermal background atmosphere. Wind shears also affect the phase difference between airglow brightness fluctuations and temperatures derived therefrom. Nonisothermal affects and the effects of diffusion and winds are largest for the slower waves we consider. Only the fastest of the ducted waves considered conform to the basic theory, while the airglow signatures associated with slower, more weakly ducted waves may be easily misinterpreted as being due to propagating waves. We conclude that for the short horizontal wavelength waves observed in the airglow, the phase of Krassovsky's ratio may be useful to identify wave ducting only for the shortest period, fastest waves. Therefore identification of ducted waves using Krassovsky's ratio will be difficult even if the required high temporal resolution measurements become available.

1. Introduction

Atmospheric gravity waves are a ubiquitous phenomenon in the atmosphere. Their importance lies primarily in their ability to transport wave energy and momentum over considerable vertical distances in the atmosphere. For high-frequency gravity waves, produced in the lower atmosphere (periods ~ 5 to 10 min, horizontal wavelengths ~ 20 km), the horizontal transport of energy and momentum is confined to a region no farther than ~ 200 km from a source. In spite of this, observations of mesospheric airglow emissions often reveal structure (bands) which apparently propagates over large horizontal distances, well in excess of 500 km or so [*Taylor et al.*, 1987, 1995; *Walterscheid et al.*, 1999; *Hecht et al.*, 2001].

Ducted waves should to be able to transport wave energy and momentum over considerable horizontal distances, and it has been suggested that they are responsible for these banded airglow features [*Taylor et al.*, 1995; *Isler et al.*, 1997; *Walterscheid et al.*, 1999; *Hecht et al.*, 2001]. However, unlike the situation for freely propagating waves, the wave energy and momentum associated with ducted waves remains trapped within a fairly narrow height range of the atmosphere and is unable to propagate to much greater altitudes. Because we need to quantify the upward transport of gravity wave energy and momentum in the upper mesosphere and lower thermosphere region in order to quantify the wave-mean flow interaction in the overlying atmosphere, being able to clearly differentiate between ducted waves and freely propagating waves using such airglow observations is an important challenge. One possible way to do this is to examine the phase differences between airglow brightness fluctuations and airglow temperature fluctuations. For the case of idealized ducting, the theory is well developed, as explained below. However, extending this theory to the more realistic case when non ideal ducting conditions prevail is a significantly more complex task for which numerical models are usually required.

Gravity waves may be strongly influenced by the effects of winds and thermal gradients as they propagate upward through the atmosphere. Gravity waves propagating in a direction normal to the mean winds are unaffected by those winds, but for different azimuths of propagation, the winds will Doppler shift the wave frequency. For an internal gravity wave propagating against a mean wind the wave frequency will be Doppler shifted to higher frequencies. In this case, if the wave period in a windless atmosphere is close to the Brunt-Väisälä period, the wind may Doppler shift the frequency into the evanescent wave regime. Alternatively, an evanescent wave propagating in the same direction as the mean wind may have its frequency Doppler shifted to lower frequencies and into the internal gravity wave regime. Because ducted waves are internal gravity waves trapped between two evanescent regions (or alternatively, trapped between the ground and an upper evanescent region), it is clear that winds are able to cause ducting of gravity waves [*Pitteway and Hines*, 1965; *Friedman*, 1966; *Hines and Reddy*, 1967; *Reddy*, 1969; *Francis*, 1973; *Chimonas and Hines*, 1986; *Isler et al.*, 1997; *Walterscheid et al.*, 1999; *Hecht et al.*, 2001].

The existence of thermal gradients implies that the Brunt-Väisälä period (τ_B) varies with altitude. In this case, a gravity

Paper number 2001JD900182.
0148-0227/01/2001JD900182$09.00

wave may be internal in the region of local minimum of τ_B, and become evanescent at some distance either side of this where τ_B has increased [*Hines*, 1960; *Wickersham*, 1968; *Walterscheid et al.*, 1999; *Hecht et al*, 2001]. In this case, the wave would be thermally ducted. Alternatively, a gravity wave may be ducted between the ground and some higher region of the atmosphere where the wave becomes locally evanescent [*Thome*, 1968; *Francis*, 1973; *Richmond*, 1978; *Tuan and Tadic*, 1982; *Mayr et al.*, 1984; *Wang and Tuan*, 1988; *Munasinghe et al.*, 1998].

Ducted waves tend to have large vertical wavelengths and so tend to be more easily observed in the airglow because cancellation effects within the airglow are then small [*Hines and Tarasick*, 1994; *Taylor et al.*, 1995; *Walterscheid et al.*, 1999]. A useful parameter to relate airglow intensity variations to temperature variations derived from the airglow is a complex quantity commonly known as Krassovsky's ratio, $<\eta>$ [see, for example, *Walterscheid et al.*, 1987, and references therein]. The modeling of $<\eta>$ has often employed an isothermal atmosphere, automatically precluding the possibility of thermal ducting. Exceptions to this include the studies of *Hines and Tarasick* [1994] and *Makhlouf et al.* [1995]. In the former analytic modeling study it was concluded that intensity and temperature fluctuations would occur either exactly in phase or exactly in antiphase for waves perfectly ducted in the airglow region. The latter numerical modeling study relied on wave reflection from the ground, so that the ducting region was very deep (~ 100 km), favoring the ducting of faster gravity waves having large vertical wavelengths. Nonetheless, the basic theory proposed by *Hines and Tarasick* [1994] was numerically confirmed.

The theory of *Hines and Tarasick* [1994] (hereinafter referred to as HT94) was suggested to help explain the observations of *Zhang et al.* [1993a, 1993b], which often revealed in-phase fluctuations of intensity and temperature. Because these small phase differences could not be explained by other models and other physical processes [e.g., *Hickey et al.*, 1993] the HT94 theory was quite a success. However, some of the observations of *Zhang et al.* [1993a] revealed small but nonzero phase differences which could not be explained by HT94. It seems clear that such disagreement is probably a result of the real atmosphere not always being able to support fully ducted waves. Instead, wave ducts are more likely to be leaky, and reflections occurring at the boundaries, separating regions of propagation from regions of evanescence, are then expected to be imperfect, a possibility that was also appreciated by HT94. In turn, this will cause modifications to the phase of Krassovsky's ratio in ways that have hitherto gone unexplored. One of the waves observed and reported by *Zhang et al.* [1993a] has been shown by *Walterscheid et al.* [2000] to be subject to strong reflection in the mesopause region, in support of HT94. This particular wave has also been studied by *Hickey* [2001] using a full-wave model.

It is the purpose of this paper to study the consequences of imperfect wave ducting on the phase of Krassovsky's ratio, $<\eta>$, by considering gravity wave propagation in a nonisothermal atmosphere that includes the diffusion of heat and momentum. We have chosen to mainly limit the range of wave parameters to those most obviously associated with band structure in the airglow and attributed to wave ducting by *Taylor et al.* [1995], *Isler et al.* [1997], *Walterscheid et al.* [1999], and *Hecht et al.* [2001]. These waves are of smaller scale than those observed by *Zhang et al.* [1993a], and we choose them because they are an almost ubiquitous feature of airglow observations.

The layout of this paper is as follows: In section 2 we review the theory of ducted waves and the effects of ducted waves on airglow variations. In section 3 we discuss the numerical model used to study the wave ducting. Results are discussed in section 4. Our first simulation is for an ideal atmosphere, and in subsequent simulations, we relax the ideal atmosphere assumptions used in the model to determine the effect on $<\eta>$. A discussion is given in section 5, and conclusions are presented in section 6.

2. Theory

Gravity waves propagating in a nonisothermal, dissipationless, and windy background atmosphere have a vertical wave number (m) presribed by the dispersion equation [*Hines*, 1960; *Einaudi and Hines*, 1971]

$$m^2 = \frac{k^2}{\Omega^2}\left(N^2 - \Omega^2\right) - \frac{1}{4H^2} + \frac{\Omega^2}{C^2}, \tag{1}$$

where k is the horizontal wave number, H is the atmospheric pressure scale height, C is the sound speed, and N is the nonisothermal Brunt-Väisälä frequency. Ω is the intrinsic (i.e., Doppler shifted) wave frequency, given by

$$\Omega = \omega - \underline{k}\cdot\underline{U}, \tag{2}$$

where ω is the extrinsic (observable) wave frequency (assumed to be much greater than the inertial frequency), $\underline{k}$ is the horizontal wave number vector, and $\underline{U}$ is the mean wind. Also,

$$N^2 = \left(\gamma - 1 + \gamma dH/dz\right)g^2/C^2. \tag{3}$$

Additional useful relations are $H = RT/Mg$ and $C^2 = \gamma gH$, where R is the universal gas constant, T is the mean temperature, M is the mean molecular weight, g is the gravitational acceleration, and γ is the usual ratio of specific heats. Also, the vertical wavelength is given by $\lambda_z = 2\pi/m$.

For both internal acoustic waves and internal gravity waves, $m^2 > 0$, while for evanescent waves, $m^2 < 0$. The last term in (1) is commonly neglected in evaluating m^2; but for very short period gravity waves, it can be easily shown that it is of comparable magnitude to the third term in (1). The third term is equal to ω_a^2/C^2, where ω_a is the acoustic cutoff frequency ($\omega_a = C/2H$). For an isothermal atmosphere composed only of diatomic gas molecules (γ = 1.4), the ratio ω_a^2/N^2 is equal to 1.225. Therefore as $\Omega \to N$, the ratio of the last term to the third term approaches 1/1.225 $\approx$ 0.82, which is non negligible.

As noted in section 1, and according to (2), an internal gravity wave ($m^2 > 0$) propagating opposite to a mean wind will have its frequency Doppler shifted to higher frequencies. As the mean wind increases, Ω increases, and m approaches zero. In the limit $\Omega = N$, $m^2 = (N^2 - \omega_a^2)/C^2$, where ω_a is the acoustic cutoff frequency as previously defined. Because $\omega_a > N$ in an isothermal atmosphere, $m^2 < 0$ when $\Omega = N$. So, depending on the value of k and the values of the atmospheric parameters appearing in (1), m^2 may eventually become negative for a large enough wind (which will occur for $\Omega > N$), leading to wave reflection.

Alternatively, an evanescent wave ($m^2 < 0$) propagating in the same direction as a mean wind will have its frequency

Doppler shifted to lower frequencies. As the mean wind increases, Ω decreases and approaches N. At $\Omega = N$, $m^2 < 0$ and the wave is still evanescent. As the mean wind increases further, $\Omega < N$, and depending on the value of k and the values of the atmospheric parameters appearing in (1), m^2 may eventually become positive, again leading to wave reflection. In the region where the winds are strong and in the same direction as the wave, the wave may be internal and therefore ducted. This is commonly referred to as Doppler ducting [*Chimonas and Hines*, 1986]. For the remainder of this paper we refer to this as "classical Doppler ducting." However, the situation of an internal gravity wave becoming locally evanescent by propagating in a direction opposite to a mean wind, as discussed in the previous paragraph, may equally be termed Doppler ducting because the ducting is facilitated by the background winds.

Thermal ducting can occur in the lower thermosphere where a local maximum in the value of N occurs. A gravity wave may be locally internal in the vicinity of this local maximum, but at some distance below and above this region where N is smaller, the gravity wave may be evanescent. Waves more likely to be thermally ducted in the lower thermosphere thermal duct have short horizontal wavelengths ($\leq$ 30 km) and short periods ($\leq$ 7 min) [*Walterscheid et al.*, 1999]. Background winds and their associated shear will modify the thermal ducting and can detune or even destroy it [*Jones*, 1972], as discussed further by *Walterscheid et al.* [1999]. In this instance the winds can remove one of the evanescent regions by locally increasing m^2. However, background winds may also strengthen the thermal ducting if the winds are in the opposite direction to the wave propagation in the region of thermal evanescence. In this case the winds would make m^2 more negative. Because the winds vary in a complicated way with local time and season (as well as other complicating variations), the strength of the thermal duct (modified by winds) will also vary in a complicated way. Extensive numerical simulations demonstrating this can be found in the work of *Hecht et al.* [2001].

Waves having large vertical wavelengths within the airglow region tend to be more easily observed because cancellation effects within the airglow are then small [*Hines and Tarasick*, 1987; *Schubert and Walterscheid*, 1988; *Swenson and Gardner*, 1998; *Hickey and Walterscheid*, 1999]. Because ducted waves have large vertical wavelengths, they also tend to be more easily observed in the airglow [HT94; *Walterscheid et al.*, 1999]. A useful parameter to relate airglow intensity variations to temperature variations derived from the airglow is Krassovsky's ratio ($<\eta>$), defined by

$$<\eta> = \left(<I'>/<\bar{I}>\right) \Big/ \left(<T_I'>/<\bar{T}_I>\right) \qquad (4)$$

[*Schubert and Walterscheid,* 1988; *Schubert et al.*, 1991]. Here the angle brackets denote an integral over the vertical extent of the emission, I is the volume emission rate, and T is the volume emission rate weighted temperature. A prime denotes a linear perturbation to the mean, which bears an overbar. One of the important aspects of $<\eta>$ as defined by (4) is that it is independent of wave amplitude. Note that the height-integrated volume emission rate is the brightness.

The response of the airglow to fully ducted waves in the atmosphere has been discussed by *Hines and Tarasick* [1994]. Fully ducted gravity waves may only exist in an "ideal" atmosphere (discussed below) and would require that an integer number of half-vertical wavelengths fit exactly into the vertical extent of the duct to minimize wave amplitudes at the duct boundaries. Unlike ducting involving a rigid boundary, true nodes do not exist at the boundaries of the ducts we consider, so the waves are not fully ducted and the half-vertical wavelength requirement is then an approximation. However, wave amplitudes can be minimized at these boundaries, and such waves are said to be resonant.

For this paper we define an "ideal" atmosphere as one that is isothermal, free of the effects of diffusion and dissipation, and where winds may exist only to bound a region of propagation from regions of evanescence. Under such conditions the phase of $<\eta>$, denoted $\varphi(\eta)$ (where for convenience we have dropped the angle brackets), defined as the phase difference between brightness fluctuations and airglow temperature fluctuations, will be either exactly zero or π. The half-vertical wavelength requirement derives strictly from the requirement that there exist nodes in the vertical velocity at the vertical extremities of the duct. However, this is not an essential requirement if the regions of evanescence bounding the duct are very deep, a situation considered later in this paper.

However, the real atmosphere is far from ideal. Background winds vary with height, as does the mean temperature. Also, waves are usually dissipated to some degree because of effects associated with the eddy and molecular diffusion of heat and momentum (the eddy diffusion being associated with much smaller scale waves and random motions). Wave-wave interactions and other nonlinear phenomena frequently occur (such as wave breaking), and although these are not considered here, they will also cause a departure from ideal behavior. Additionally, in general, the combination of wave parameters will be such that an integer number of half-vertical wavelengths do not fit exactly into the vertical extent of the duct. All of these conspire to make the atmosphere behave in a way that is unlikely to support fully ducted waves. In fact, although the theory presented by *Hines and Tarasick* [1994] went a long way toward explaining the observations of *Zhang et al.* [1993a, 1993b], it is not surprising that it could not explain all of them. Negative values of $\varphi(\eta)$ are also indicative of strong reflection [*Hines and Tarasick*, 1994], which may explain the observations of long period waves in the OI 5577Å airglow described by *Schubert et al.* [1999] [see also *Walterscheid et al.*, 2000].

To test the HT94 theory, one could compare the value of $\varphi(\eta)$ obtained for the case of classical Doppler ducting with the value of $\varphi(\eta)$ obtained by ignoring wind effects, in both cases for an otherwise ideal atmosphere. In the former case, the HT94 theory tells us that $\varphi(\eta)$ will be either zero or π. However, the same results would also be obtained in the windless case. The reason for this is that for classical Doppler ducting the wind serves only to modify an evanescent wave such that it becomes internal (propagating) in the region of maximum wind. Therefore in the absence of winds the wave remains evanescent. However, evanescent waves have very large (ideally infinite) vertical wavelengths, λ_z, and they too will have values of $\varphi(\eta)$ equal to either zero or π. Therefore comparing the values of $\varphi(\eta)$ obtained for classical Doppler ducting with those obtained without winds is ambiguous and not a suitable test of HT94. The situation would become more difficult when we consider a non ideal atmosphere, as we wish to do. Therefore in this paper we consider the other form of Doppler ducting discussed at the start of this section,

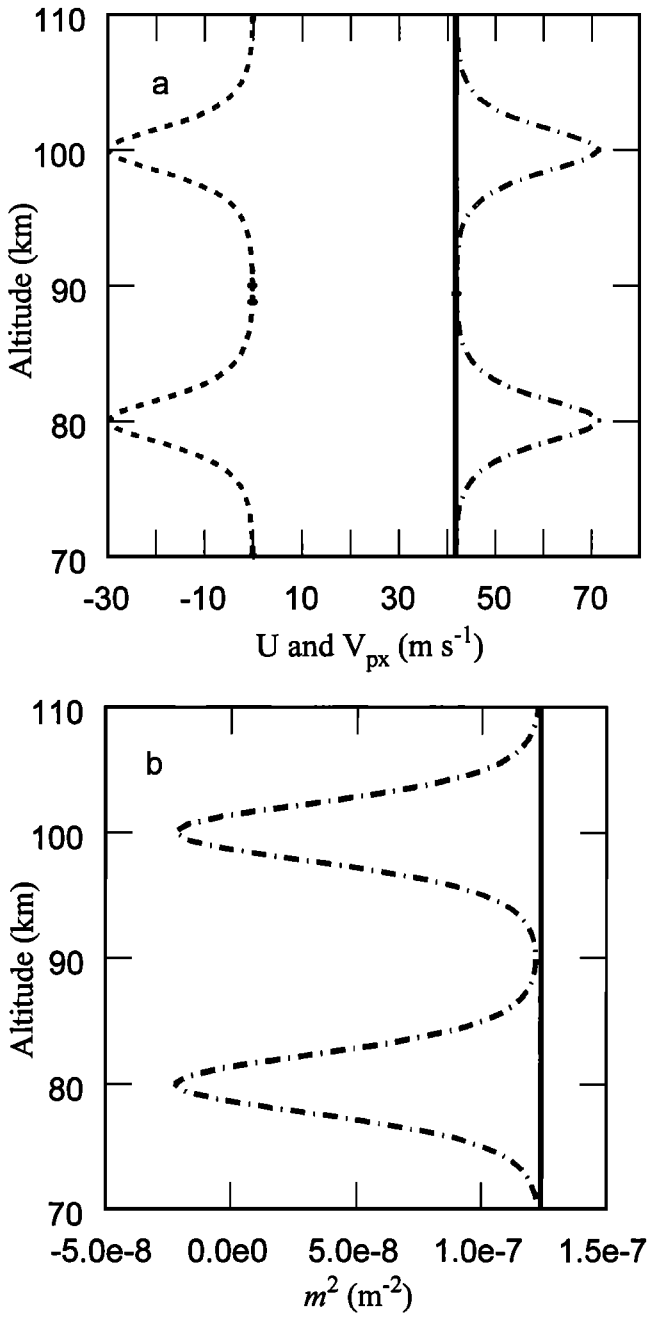

Figure 1. (a) A simple wind profile (dashed curve), the corresponding wave extrinsic phase speed (solid line), and the wave intrinsic phase speed with respect to the wind (dashed-dotted curve); (b) the refractive index calculated without a mean wind (solid curve) and calculated using the mean wind shown in Figure 1a (dashed-dotted curve). See text for details.

wherein the wind direction is opposite to that of the phase propagation of the gravity waves.

The relevant situation is depicted in Figure 1. Here we consider a wave of an extrinsic period of 8 min and a horizontal wavelength of 20 km (with an extrinsic phase speed v_{px} of ~ 42 m s^{-1}) propagating in an isothermal atmosphere with a constant Brunt-Väisälä period (τ_g) of 5 min. We use a wind profile that is not representative of the real atmosphere but which serves well to illustrate the ducting principle. The wind profile is such that in the region near 90 km altitude, and at the lowest and highest altitudes shown (70 km and 110 km, respectively), the mean wind is ~ zero. The wind achieves a maximum speed (in a direction opposite to v_{px}) of -30 m s^{-1} at 80 km and 100 km altitude (Figure 1a, dashed curve). In the case of no wind, the intrinsic phase speed equals the extrinsic phase speed and does not vary with height (solid line). In the case with winds (dashed-dotted curve) the intrinsic phase speed is height dependent and becomes large in the region of strongest winds. The corresponding refractive index, m^2 (the square of the vertical wave number as given by equation (1)), is shown in Figure 1b. In the no wind case, m^2 does not vary with height and is positive at all heights signifying internal wave propagation. However, in the case with winds it varies with height and becomes negative in the regions of maximum (negative) winds, signifying evanescence in these regions. In the region of small winds near 90 km altitude, m^2 is positive, signifying internal wave propagation. This is the ducting region, and it is this mechanism for wave ducting that we consider for the remainder of this paper.

2.1. Model

To calculate $\varphi(\eta)$ for an atmosphere including winds, diffusion, and height variations of mean temperature, we employ a full-wave model that has been described by *Hickey et al.* [1997, 1998, 2000]. The model solves the linearized Navier-Stokes equations for steady state waves propagating in a nonisothermal atmosphere, including horizontal mean winds and the eddy and molecular diffusion of heat and momentum. The lower boundary is the ground, and the upper boundary, for these simulations was set to 400 km altitude. We used 120,000 grid points in the vertical, corresponding to a height resolution of 3.3 m.

Boundary conditions have been extensively discussed in the above full-wave model references. Essentially, the ground reflects waves, and at the upper boundary, a radiation condition is applied, using a dispersion equation given by *Hickey and Cole* [1987]. A sponge layer is also implemented at the upper boundary to absorb any waves that may be reflected due to a slight mismatch between full-wave and WKB-type solutions used during the implementation of the radiation condition [*Hickey et al.*, 2000].

In addition to the obvious advantage of being able to include several important physical processes in our full-wave model simulations, the model also allows us to simulate wave ducting without having to explicitly specify any boundary conditions associated with the boundaries of the duct. *Richmond* [1978] has discussed the subtleties associated with boundary conditions related to wave ducting. Reflection processes in the thermosphere associated with height variations of kinematic viscosity and molecular weight, as well as ground reflection in the lower atmosphere, all modify the ducted wave solutions and require treating the boundary conditions at the duct walls very carefully. However, in our model the resulting wave solutions within the ducted region already include all of these effects, and there is no need to prescribe any specific boundary conditions related to the existence of a duct.

The full-wave model outputs altitude profiles of amplitude and phase for the horizontal velocity components (u' and v'), the vertical velocity (w'), the temperature perturbation (T'), and the pressure perturbation (p'). These are input to a steady state model describing fluctuations in the O_2 atmospheric airglow emission, which has been discussed by *Hickey*

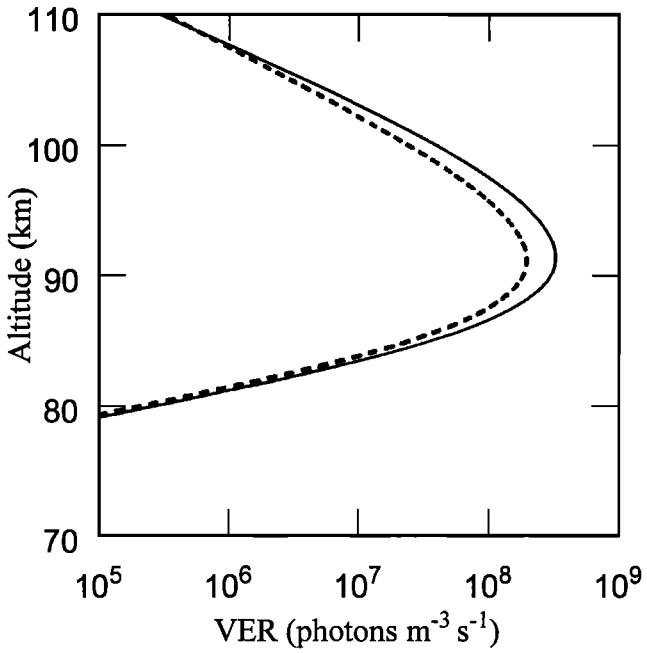

Figure 2. Mean O_2 atmospheric nightglow volume emission rate calculated using the chemical kinetic parameters provided by *Hickey et al.* [1993] and *Hickey and Walterscheid* [1999] for an isothermal atmosphere (dashed curve) and a nonisothermal atmosphere (solid curve).

et al. [1993] and updated by *Hickey and Walterscheid* [1999]. The final airglow model output is the amplitude and phase of $<\eta>$. The undisturbed profile of the volume emission rate (VER) is shown in Figure 2, for both an isothermal atmosphere (solid curve) and a nonisothermal atmosphere (dashed curve). The VER peaks near 91.2 (91.4) km altitude with a value of 1.94 x 10^8 (3.3 x 10^8) photons m^{-3} s^{-1} for the isothermal (nonisothermal) atmosphere. The mean temperature is shown in Figure 3. The mesopause is fairly broad, with the minimum value of ~180 K occurring at ~ 95 km altitude, which is about 4 km above the altitude of peak VER.

To quantify the efficiency of the wave ducting, we also examine the phase difference between vertical velocity perturbations and pressure perturbations, which we denote $\varphi(w'p')$. For perfect ducting, one expects no vertical transport of energy within the duct, so w' and p' are in phase quadrature and $\varphi(w'p') = \pm\pi/2$. Large departures of $\varphi(w'p')$ from a value of $\pm\pi/2$ signify inefficient ducting or, in the extreme, a complete lack of ducting. Therefore based on HT94, we expect values of $\varphi(\eta)$ very close to either zero or π should be associated with values of $\varphi(w'p')$ very close to $\pm\pi/2$. Unless stated otherwise, we calculate an average value of $\varphi(w'p')$ between altitudes of 80 km and 110 km. In a nonisothermal atmosphere and for propagating (nonevanescent) waves having a horizontal wavelength of 20 km, we obtain values of $\varphi(w'p')$ which increase from about 1.5° to 10.6° as the wave period decreases from 20 min to 6 min. Note that our measure of wave ducting, based on the phase quadrature of w' and p', may not be the best measure in the case of strong sheared flow because then the vertical energy flux is not necessarily zero [*Holton*, 1975, p.107].

3. Results

In this section we use the full-wave model to determine both $\varphi(\eta)$ and $\varphi(w'p')$ for a fixed horizontal wavelength (λ_x) of 20 km and for 100 different wave periods ranging from 5.5 min to 20 min. The value of λ_x is representative of waves that are prevalent in the airglow and which are expected to be associated with ducted waves [*Taylor and Hapgood.*, 1990; *Taylor et al.*, 1995; *Isler et al.*, 1997; *Walterscheid et al.*, 1999; *Hecht et al*, 2001]. We perform simula-

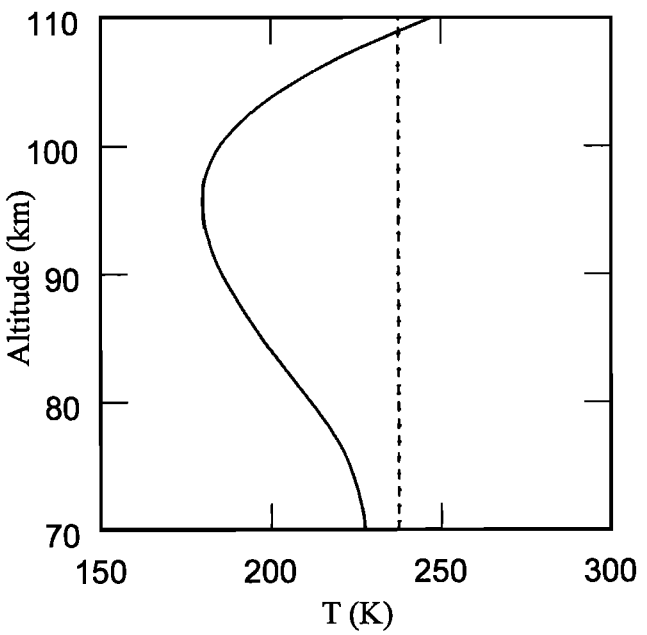

Figure 3. Mean atmospheric temperature used in the computations for an isothermal atmosphere (dashed line) and a nonisothermal atmosphere (solid curve).

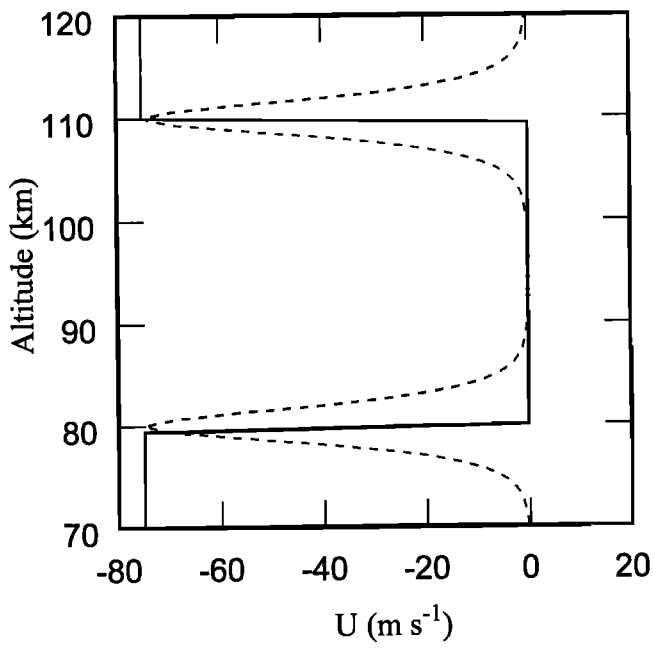

Figure 4. Nominal mean winds used in the simulations: a square wind profile (solid lines), and a wind profile constructed using two hyperbolic secant profiles (dashed curve).

tions for various types of atmospheric conditions, which are discussed separately in each of the following subsections.

For the results shown in sections 3.1 to 3.4 we impose a background wind with a square profile shape, such that $\bar{U}$ is zero between 80 km and 110 km altitude and is –75 m s^{-1} otherwise (solid lines, Figure 4). Therefore the waves are internal over the 30 km region of the duct between 80 and 110 km and are evanescent at all other altitudes. For the results shown in section 3.5 we impose the wind profile shown as the dashed curve in Figure 4. These winds are a composite of two hyperbolic secant profiles, each with a full width at half maximum of 4 km and a maximum speed of –75 m s^{-1}, and each centered on 80 km and 110 km, respectively. The vertical extent of the duct in this case is a function of wave phase speed. For both sets of wind profiles shown in Figure 4 the region of small winds at 95 km altitude is approximately 4 km above the region of peak VER shown in Figure 2.

The nominal eddy diffusion coefficients are based upon a profile due to *Strobel* [1989] and have large values in the airglow region (see Figure 5). The Prandtl number is equal to 3 for these simulations. In addition to using the nominal model diffusion coefficients, we also consider the case of significantly reducing all model diffusion coefficients in order to approximate a dissipationless atmosphere (which we term quasi-adiabatic). In particular, the molecular diffusion coefficients are reduced by a factor of 10^4 from their nominal values, and the eddy diffusion profile is taken to be constant in altitude with a value of 0.1 m^2 s^{-1}. It is important to realize that diffusion cannot be completely omitted in this numerical model because the set of second-order differential equations (DEs) would then essentially reduce to a set of first-order DEs, providing a singularity in the system behavior.

3.1. Isothermal, Quasi-Adiabatic Ducting

In this case the atmosphere is taken to be isothermal with a mean temperature of 237.6 K, and diffusion coefficients are reduced from their nominal values as discussed above. The phase difference between w' and p', $\varphi(w'p')$, is shown as the solid line in Figure 6. For the lower frequency and slower waves, $\varphi(w'p')$ is less than $\pi/2$, but it always exceeds ~ 80° (which is almost 90% of the value $\pi/2$). As frequency and phase speed both increase, $\varphi(w'p')$ smoothly approaches the value of $\pi/2$. The phase of Krassovsky's ratio, $\varphi(\eta)$, is shown as the short-dashed curve in Figure 6. It varies between approximately zero and π as wave frequency increases, as predicted by HT94. For the lower frequency and slowest waves, $\varphi(\eta)$ deviates from zero by a small but perceptible amount compared to values of $\varphi(\eta)$ which are closer to zero for the higher frequency, faster waves.

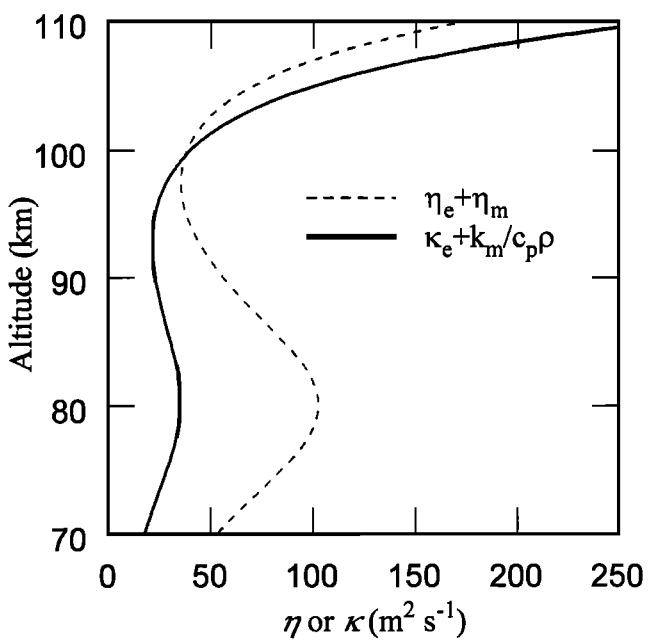

Figure 5. Nominal eddy and molecular momentum (dashed curve) and thermal (solid curve) diffusivities used in the simulations.

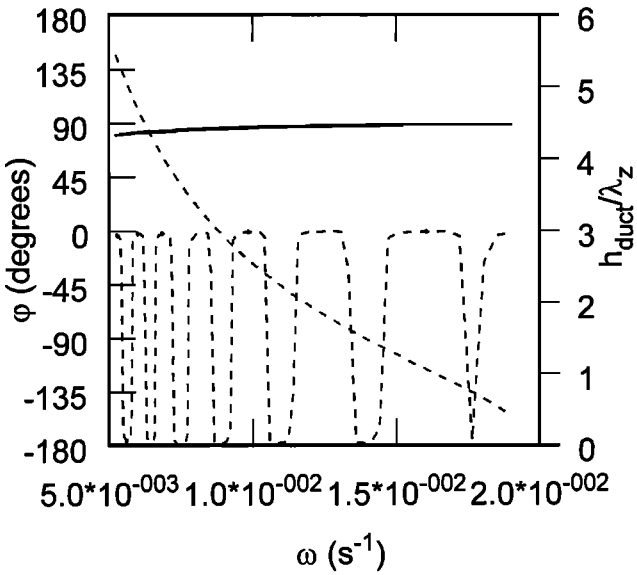

Figure 6. Average phase difference between w' and p' (solid line), phase of $<\eta>$ (thick dashed curve), and the ratio of the duct depth to the vertical wavelength of an equivalent freely propagating wave (thin dashed curve), plotted as a function of wave frequency, for an isothermal, adiabatic atmosphere, and with the square wind profile. See text for details.

Also shown in Figure 6 is the ratio (h_{duct}/λ_z) of the depth of the duct (h_{duct} = 110-80 = 30 km) to the vertical wavelength (λ_z) calculated using the dispersion equation of *Hines* [1960] (this ratio is scaled to the right-hand vertical axis in the figure). We include this result in the isothermal, quasi-adiabatic case only because under these conditions the dispersion equation provides a good estimate of the vertical wavelength (λ_z) within the duct. For almost the highest-frequency gravity wave (corresponding to T ~ 5.5 min), half of a vertical wavelength fits into the duct (the fundamental vertical wavelength ~ 2 x 30 = 60 km). As wave frequency is reduced, λ_z decreases, and h_{duct}/λ_z increases. A comparison of the h_{duct}/λ_z curve with the $\varphi(w'p')$ curve shows that the ducting becomes more efficient for the higher frequency, faster waves for which λ_z is an appreciable fraction of h_{duct}.

3.2. Nonisothermal, Quasi-Adiabatic Ducting

In this case the mean temperature varies with altitude (see Figure 3, solid curve). The diffusion coefficients used in the model are the same as those used in section 3.1. Results are shown in Figure 7. The nonisothermal character of the atmosphere has a stronger mitigating effect on the ducting effi-

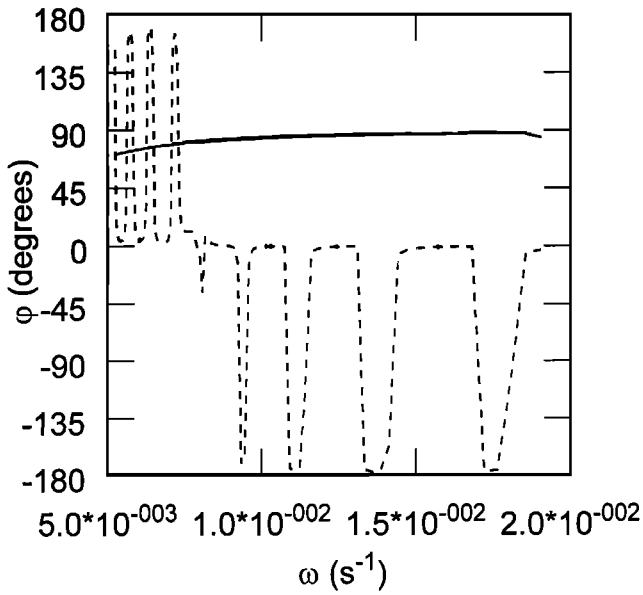

Figure 7. Similar to the results shown in Figure 6 except for a nonisothermal, adiabatic atmosphere. The duct depth/vertical wavelength ratio is not shown (or calculated) in this case.

ciency of the atmosphere for the lower frequency, slower waves, for which the quantity $\varphi(w'p')$ is significantly reduced over its corresponding isothermal values. The higher frequency, faster waves are not significantly affected by the change from an isothermal to a nonisothermal atmosphere, except for the very fastest, largest vertical wavelength waves.

For the slower waves, $\varphi(\eta)$ is positive (and less than π), and airglow temperature variations lead intensity variations for these waves. For the faster waves, $\varphi(\eta)$ varies between about zero and π. For the faster waves the nonisothermal character of the atmosphere has affected $\varphi(\eta)$ in a small but noticeable way, which can be seen by comparing the proximity of $\varphi(\eta)$ to either zero and π for this case and for the results shown in Figure 6 (section 3.1).

3.3. Isothermal, Nonadiabatic Ducting

In this case we use the same constant temperature profile used in section 3.1, and the nominal eddy and molecular diffusion coefficients. Figure 8 shows both $\varphi(w'p')$ and $\varphi(\eta)$ plotted as a function of wave frequency. A noticeable feature of these results is that $\varphi(w'p')$ departs significantly from $\pi/2$ for the lower frequency, slower waves. This is expected because the slower waves are more susceptible to the effects of dissipation, which alters the phase relations between the different perturbation components of the wave. This then leads to an increased leakage of energy from the duct and less efficient ducting. As wave frequency increases, $\varphi(w'p')$ smoothly increases and approaches a value close to $\pi/2$.

Another noticeable feature of the results is that $\varphi(\eta)$ varies between zero and π (the latter only approximately so) only for the higher frequency, faster waves. For the lower frequency and slower waves, $\varphi(\eta)$ differs significantly from either zero or π due to the effects of dissipation. Dissipation alters the relative phases between the various wave components, as mentioned in the previous paragraph. Additionally, dissipation can also alter the phase relation between the perturbation temperature and the minor species perturbations [*Hickey*, 1988a, 1988b]. It is these combined effects of dissipation that lead to significant differences between $\varphi(\eta)$ calculated with and without dissipation. For the higher-frequency waves less affected by dissipation there is a clear association between the occurrence of values of $\varphi(\eta)$ close to zero or π and the occurrence of values of $\varphi(w'p')$ close to $\pi/2$.

3.4. Nonisothermal, Nonadiabatic Ducting

In this case we use the temperature profile described in section 3.2 and the nominal eddy and molecular diffusion coefficients. The results are presented in Figure 9. Values of $\varphi(w'p')$ differ dramatically from $\pi/2$ for the lower frequency, slower waves, and approach values associated with freely propagating waves. It is only for the high frequency, fast waves ($\omega \geq 1.2 \times 10^{-2}$ s^{-1}, or $V_{px} \geq 38$ m s^{-1}) that the value of $\varphi(w'p')$ approaches $\pi/2$. However, for the very fastest, highest-frequency waves, $\varphi(w'p')$ decreases. For the low frequency, slower waves, the values of $\varphi(\eta)$ are very different than those obtained for ideal ducted waves. This is not completely surprising, because the $\varphi(w'p')$ results suggest that these waves are more freely propagating and that ducting is very inefficient. As frequency increases, and ducting becomes stronger (as based on the behavior of $\varphi(w'p')$), $\varphi(\eta)$ behaves more in a way that is associated with ducted waves. The transition from nonducting behavior to ducting behavior is gradual and occurs in a way that cannot be easily predicted without recourse to extensive numerical modeling. The $\varphi(\eta)$ value exhibits behavior associated with ducting for wave frequencies greater than about 1.2×10^{-2} s^{-1} ($T \leq 8.7$ min and $V_{px} \geq 38$ m s^{-1}), which coincides with values of $\varphi(w'p')$ of about 76° (or about 84% of the value of $\pi/2$).

3.5. Nonisothermal, Nonadiabatic Ducting in a Simple Mean-Shear Wind Profile

In this case we use the temperature profile described in section 3.2 and the nominal eddy and molecular diffusion coefficients. We also use the nonidealized mean wind profile, based on the hyperbolic secant profiles discussed earlier and

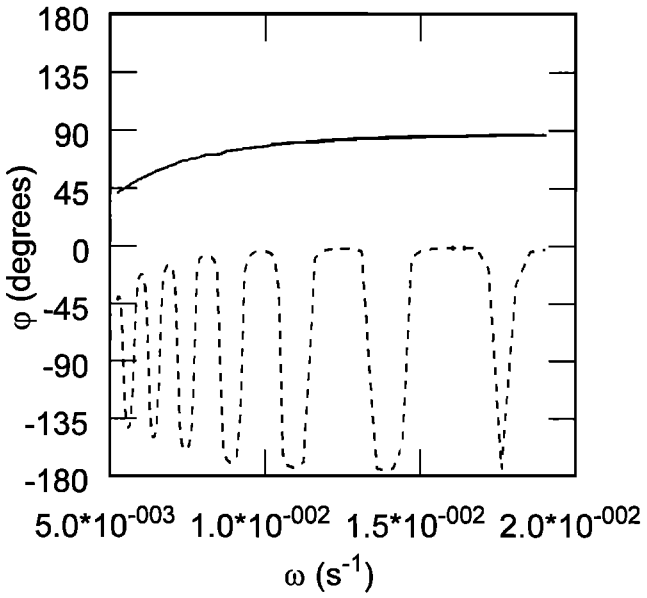

Figure 8. Similar to the results shown in Figure 7 except for an isothermal, nonadiabatic atmosphere.

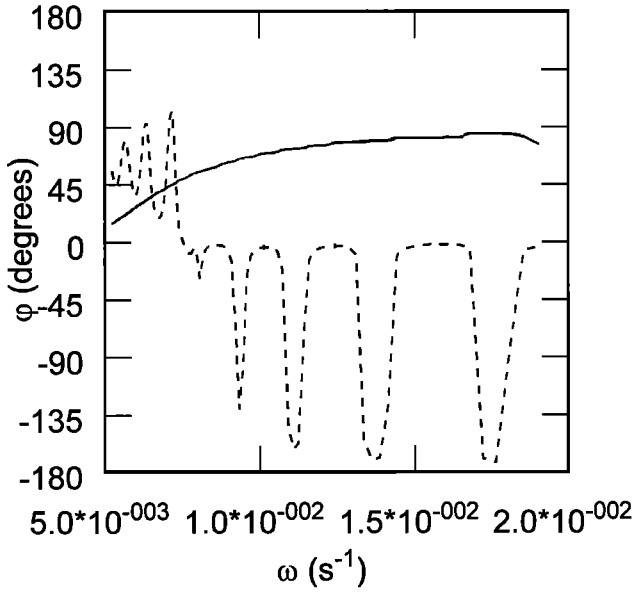

Figure 9. Similar to the results shown in Figure 7 except for a nonisothermal, nonadiabatic atmosphere.

shown in Figure 4 (dashed curves). Unlike the ducts considered in sections 3.1 to 3.4, the vertical extent of this duct is a function of wave phase speed. The duct is deeper for the slower waves (with a maximum depth of almost 20 km) and shallower for the faster waves. An additional difference between the wind profile and the idealized square wind profile is that in the latter case, the evanescent regions were very thick (many tens of kilometers) whereas in the present case, the evanescent regions are fairly thin (a few kilometers for the faster waves and ~ 10 km for the slower waves). Therefore the strength of the ducting is much weaker when the hyperbolic secant wind profiles shown in Figure 4 are used because significant tunneling of wave energy is possible through the thin evanescent regions. Because the duct considered here is much narrower in vertical extent than the duct previously considered, we calculate an average value of $\varphi(w'p')$ over the height interval 92 km to 98 km.

The $\varphi(w'p')$ results (Figure 10, solid curve) show that the slower waves exhibit no signs of ducting behavior. Compared to ducted waves, these slower waves with $\omega \leq 1.25 \times 10^{-2}$ s^{-1} have relatively large vertical fluxes of energy and momentum. The faster waves (those at greater frequencies than this) exhibit signs of ducting behavior for certain frequency ranges as a consequence of the requirement that an integer number of half-vertical wavelengths fit into the vertical extent of the duct. Vertical wavelength is not constant throughout the vertical extent of the duct, but the above requirement is matched more closely for those waves for which $\varphi(w'p')$ is a local maximum on the frequency axis. For the fastest waves, ducting is more efficient because the vertical wavelengths are greater and match the vertical extent of the duct more closely. Additionally, the faster waves experience the least dissipation.

The $\varphi(\eta)$ results (dashed curve) show that the slower waves exhibit no signs of ducting, while faster waves with $\omega \geq 1.0 \times 10^{-2}$ s^{-1} exhibit some signs associated with weak ducting. For the faster waves there is a tendency for $\varphi(\eta)$ to vary between a local minimum and a local maximum as a function of frequency, but the local maximum only approaches zero for the fastest waves. The local minimum never achieves a value very close to $-\pi$. Overall, the use of a wind profile having smooth height derivatives, as well as a more realistic mean state atmosphere (nonisothermal and including effects of dissipation), has severely degraded the ability of the atmosphere to duct the waves, at least as far as derived values of $\varphi(\eta)$ are concerned.

4. Discussion

Currently, the temporal resolution of airglow imaging devices is a few minutes (M.J. Taylor, private communication, 2000; J.H. Hecht, private communication, 2000). To determine values of $<\eta>$ for ducted waves, with observed periods of ~ 5 min or less, a single intensity measurement and a single temperature measurement both need to be determined within ~ 2 min or less. In order that accurate phase differences between a derived intensity and temperature time series can be determined, more frequent sampling would be required. Therefore although, in principal, the phase of $<\eta>$ ($\varphi(\eta)$) can be used to determine if the very short period and short wavelength waves often seen in the airglow are in fact ducted, technological restrictions preclude such a determination at this time. However, with technological advances we expect that $\varphi(\eta)$ may become a very useful quantity to assess the role of ducting in future observations.

In the event that $\varphi(\eta)$ can be determined for short-period waves observed in the airglow, favorable comparison with the HT94 theory, which is applicable to an idealized atmosphere, cannot always be expected. Significant departures from the HT94 theory can always and should always be expected for slower waves (in this case, waves satisfying $V_{px} \leq 38$ m s^{-1}). Many of the waves identified by *Walterscheid et al.* [1999] and by *Hecht et al.* [2001] had horizontal phase speeds com-

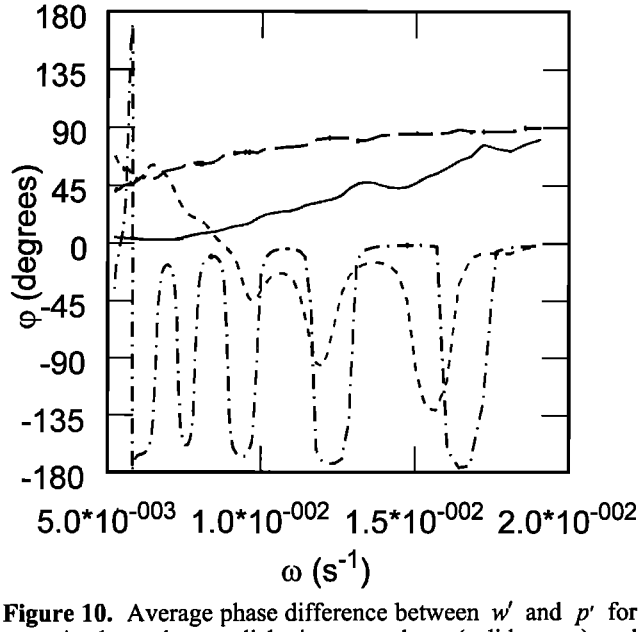

Figure 10. Average phase difference between w' and p' for a nonisothermal, nonadiabatic atmosphere (solid curve) and for an isothermal, adiabatic atmosphere (long-dashed curve), and phase of $<\eta>$ for a nonisothermal, nonadiabatic atmosphere (thick short-dashed curve) and for an isothermal, adiabatic atmosphere (dashed-dotted curve), and with the hyperbolic secant wind profile. See text for details.

parable to or smaller than this, and so our modeling implies that $\varphi(\eta)$ for these waves may not conform to the HT94 theory.

We have performed simulations for a single value of horizontal wavelength (20 km). This value appears to be more typical of waves believed to be ducted [*Isler et al.*, 1997; *Walterscheid et al.*, 1999; *Hecht et al.*, 2001]. Using larger values of λ_x (such as 30 km) would not significantly alter our conclusions. Deviations of $\varphi(\eta)$ from the HT94 theory may then be expected to occur at longer wave periods, based on the approximate phase velocity at which such deviations occurred in our present simulations (λ_z and effects of dissipation, for example, both tend to depend more on phase speed).

We have not performed simulations using either measured winds or using winds based on either numerical or empirical models. Climatological wind profiles have been used previously in wave-ducting simulations using our full-wave model by *Hecht et al.* [2001]. These wind profiles combined empirical winds [*Hedin et al.*, 1996] with a wind climatology for Urbana, Illinois, based on University of Illinois MF radar measurements (a good discussion of the MF radar winds is given by *Franke and Thorsen* [1993]). It was determined that the winds weakened (strengthened) the ducting, if the wave kinetic energy density in the region of the lower thermospheric duct decreased (increased). These wind effects were found to depend on season and local time, as well as on the particular set of wave parameters used in the simulations. In contrast to that study, the fairly simple wind profiles that we have adopted in the present study serve only to facilitate wave ducting and to help provide a clear association between the strength of the ducting and the phase of Krassovsky's ratio. Specifically, we used a hypothetical square wind profile as a means to differentiate between the waves that were locally internal within the duct and the waves that would otherwise have been evanescent throughout the entire vertical extent of the atmosphere. We also considered a smooth, continuous wind profile, to assess the effects of wind shears on the efficiency of the ducting and the phase of Krassovsky's ratio. However, neither of these wind profiles can be considered realistic and, obviously, much more modeling needs to be performed in order for us to draw any general conclusions regarding the effect of winds on the phase of Krassovsly's ratio. More realistic winds have been considered by *Hickey* [2001] in an analysis of wave reflection and the effect on airglow variations. Additional work is currently in progress using the same winds used by *Hecht et al.* [2001] in order to examine seasonal and local time variations of the phase of Krassovsky's ratio for ducted waves.

The definition of $<\eta>$ that we used, and given by equation (4), assumes that the temperature derived from an airglow measurement is a brightness-weighted temperature. As discussed extensively by *Makhlouf et al.* [1995], temperatures derived from instrument measurements often yield either a Doppler temperature or a rotational temperature, and the brightness-weighted temperature therefore represents an approximation to these. The model results of *Makhlouf et al.* [1995], which pertain to the OH nightglow, suggest that the use of a brightness-weighted temperature will lead to values of $\varphi(\eta)$ which are several degrees smaller than those obtained using either the Doppler temperature or the rotational temperature. Because O_2 atmospheric simulations were not performed by them, it is unclear how our results would be affected by the use of a different temperature formulation. *Hines and Tarasick* [1994] based their analytic formulation and derived predictions for $\varphi(\eta)$ on a brightness-weighted temperature, so comparison of our results with their predictions is completely justified.

The use of our numerical model to perform these wave ducting and airglow simulations allowed us to include realistic altitude profiles of mean temperature and diffusion coefficients that would be difficult using analytic-based models. There was no need to invoke artificial boundary conditions at the boundaries of the duct, because both the ducting region and the evanescent regions are well characterized by the model. The use of a lower, rigid boundary (the ground) is realistic, while the use of the radiation condition at very high thermospheric altitudes (~ 400 km) is also realistic. Neither the lower boundary condition nor the upper boundary condition is artificially constrained by the existence of the duct in the upper mesosphere and lower thermosphere region.

In section 2 we briefly discussed the requirement that an integer number of half-vertical wavelengths fit exactly within the vertical extent of the duct in order for nodes to exist at the duct boundaries. The existence of such nodes would serve to strengthen the ducting. However, the square wind profile used for the results presented in sections 3.1 to 3.4 created deep regions of evanescence on either side of the internal wave region of the duct. In this case the wave kinetic energy (not shown) decreased by an order of magnitude across the boundaries of the duct over a region 1–2 km thick, essentially independent of the vertical wavelength. This indicates strong trapping of wave kinetic energy within the confines of the duct. Therefore for the square wind profile the existence of nodes at the duct boundaries is not an essential requirement for strong ducting. In the case of the wind profile having nonzero shear, considered in section 3.5, the regions of evanescence are not deep, and consequently, the wave kinetic energy (not shown) is not strongly confined to the region of the duct. For an isothermal and adiabatic atmosphere this leads to a significant difference between results obtained for the two different wind profiles (compare the results shown in Figures 6 and 10). We note that the two wind profiles we have considered represent extremes in the sense that the regions of evanescence on either side of the duct are either very deep or very shallow. We expect a more realistic wind profile to have regions of evanescence of depth lying between these extremes and therefore to facilitate ducting with an efficiency lying between our two extremes. As stated earlier in this discussion, additional work is in progress assessing the impact of realistic wind profiles and their variability on the efficiency of wave ducting and its relation to the phase of Krassovsky's ratio.

The dynamical (full wave) and chemistry models are both linear, steady state models. However, the real atmosphere is more characterized by transient gravity wave packets interacting with the airglow to produce a nonlinear response [*Hickey et al.*, 2000b; *Hickey and Walterscheid*, 2001]. In this case we may expect that the airglow response would be less ideal than that of HT94. However, time-dependent, nonlinear effects with respect to wave ducting will be studied at a later time.

5. Conclusion

We have used a numerical full-wave model combined with a steady state model of the airglow response to gravity waves to simulate the airglow response to ducted waves in the upper

mesosphere and lower thermosphere region. By considering a single value of horizontal wavelength that is representative of structure seen in airglow observations and that is attributed to ducted waves, we have investigated how the strength of the ducting and the airglow response depends on wave frequency and on the properties of the atmosphere.

The strongest wave ducting occurs in an isothermal atmosphere that is free of the effects of dissipation. Under such conditions the theory of *Hines and Tarasick* [1994] is applicable, and airglow intensity fluctuations occur either exactly in phase or exactly out of phase with corresponding airglow temperature fluctuations. However, the nonisothermal nature of the atmosphere combined with the effects of eddy and molecular diffusion significantly weakens the wave ducting, due to significant departures from phase quadrature of pressure and vertical velocity fluctuations. These effects cause airglow intensity and airglow temperature to vary in a way not in accord with the theory of *Hines and Tarasick* [1994] for waves slower than about 40 m s^{-1}. Observations of banded structure in the airglow typically exhibit phase speeds no larger than this, suggesting that modeling is required to correctly interpret phase differences between intensity and temperature fluctuations inferred from observations.

Winds also affect the nature of the ducting. The square wind profile that we used provided deep regions of evanescence on either side of the duct, aiding the ducting process. The wind profile that had smooth height derivatives produced fairly narrow regions of evanescence at the duct boundaries and could not support strongly ducted waves. This has implications for ducting in the mesosphere/lower thermosphere region of the atmosphere, although a thorough analysis of wind effects needs to be performed. Based on these limited results, it appears that the phase of Krassovsky's ratio may seldom conform to the theory of *Hines and Tarasick* [1994]. The exception to this is for the fastest ducted waves ($\geq$ 50 m s^{-1} in this study), for which the phase of Krassovsky's ratio is usually close to zero or π. Therefore identification of ducted waves using airglow measurements to determine the phase of Krassovsky's ratio and to compare this value to either zero or π will be challenging and perhaps difficult at best. Given the temporal measurement constraints required to affect this for short-period waves makes this task even more daunting. For short horizontal wavelength gravity waves, it is only for the very shortest period waves that the phase of Krassovsky's ratio may be useful to identify wave ducting in the lower thermospheric duct.

Acknowledgments. MPH was supported by NSF grant ATM-9816159 to Clemson University. The comments of the referees are gratefully acknowledged.

References.

Chimonas, G., and C. O. Hines, Doppler ducting of atmospheric gravity waves, *J. Geophys. Res., 91*, 1219, 1986.

Einaudi, F., and C. O. Hines, WKB approximation in application to acoustic-gravity waves, *Can. J. Phys., 48*, 1458, 1971.

Francis, S. H., Acoustic-gravity modes and large-scale travelling ionospheric disturbances of a realistic dissipative atmosphere, *J. Geophys. Res., 78*, 2278, 1973.

Franke, S. J., and D. Thorsen, Mean winds and tides in the middle atmosphere at Urbana (40°N, 88°W) during 1991-1992, *J. Geophys. Res., 98*, 18,607-18,615, 1993.

Friedman, J. P., Propagation of internal gravity waves in a thermally stratified atmosphere, *J. Geophys. Res., 71*, 1033, 1966.

Hecht, J. H., R. L. Walterscheid, M. P. Hickey, and S. J. Franke, Climatology and modeling of quasi-monochromatic atmospheric gravity waves observed over Urbana Illinois, *J. Geophys. Res., 106*, 5181-5195, 2001.

Hedin, A. E., et al., Empirical wind model for the upper, middle, and lower atmosphere, *J. Atmos. Sol. Terr. Phys., 58*, 1421, 1996.

Hickey, M. P., Effects of eddy viscosity and thermal conduction and Coriolis force in the dynamics of gravity wave-driven fluctuations in the OH nightglow, *J. Geophys. Res., 93*, 4077, 1988a.

Hickey, M. P., Wavelength dependence of eddy dissipation and Coriolis force in the dynamics of gravity wave-driven fluctuations in the OH nightglow, *J. Geophys. Res., 93*, 4089, 1988b.

Hickey, M. P., Reflection of a long period gravity wave observed in the nightglow over Arecibo on May 8-9, 1989?, *J. Geophys. Res.*, in press, 2001.

Hickey, M. P., and K. D. Cole, A quartic dispersion equation for internal gravity waves in the thermosphere, *J. Atmos. Sol. Terr. Phys., 49*, 889, 1987.

Hickey, M. P., and R. L. Walterscheid, A note on gravity wave-driven volume emission rate weighted temperature perturbations inferred from O_2 atmospheric and O I 5577 airglow observations, *J. Geophys. Res., 104*, 4279, 1999.

Hickey, M. P., and R. L. Walterscheid, Secular variations of OI 5577 Å airglow in the mesopause region induced by transient gravity wave packets, *Geophys. Res. Lett., 28*, 701-704, 2001.

Hickey, M. P., G. Schubert, and R. L. Walterscheid, Gravity wave-driven fluctuations in the O_2 atmospheric (0-1) nightglow from an extended, dissipative emission region, *J. Geophys. Res., 98*, 13,717, 1993.

Hickey, M. P., R. L. Walterscheid, M. J. Taylor, W. Ward, G. Schubert, Q. Zhou, F. Garcia, M. C. Kelley, and G. G. Shepherd, Numerical simulations of gravity waves imaged over Arecibo during the 10-day January 1993 campaign, *J. Geophys. Res., 102*, 11,475, 1997.

Hickey, M. P., M. J. Taylor, C. S. Gardner, and C. R. Gibbons, Full-wave modeling of small-scale gravity waves using Airborne Lidar and Observations of the Hawaiian Airglow (ALOHA-93) O(^{1}S) images and coincident Na wind/temperature lidar measurements, *J. Geophys. Res., 103*, 6439, 1998.

Hickey, M. P., R. L. Walterscheid, and G. Schubert, Gravity wave heating and cooling in Jupiter's thermosphere, *Icarus, 148*, 266-281, 2000a.

Hickey, M. P., R. L. Walterscheid, and P. G. Richards, Secular Variations of Atomic Oxygen in the Mesopause Region Induced by Transient Gravity Wave Packets, *Geophys. Res. Lett., 27*, 3599-3602, 2000b.

Hines, C. O., Internal gravity atmospheric waves at ionospheric heights, *Can. J. Phys., 38*, 1441, 1960.

Hines, C. O., and C. A. Reddy, On the propagation of atmospheric gravity waves through regions of wind shear, *J. Geophys. Res., 72*, 1015, 1967.

Hines, C. O., and D. W. Tarasick, On the detection and utilization of gravity waves in airglow studies, *Planet. Space Sci., 35*, 851, 1987.

Hines, C. O., and D. W. Tarasick, Airglow response to vertically standing gravity waves, *Geophys. Res. Lett., 21*, 2729, 1994.

Holton, J. R., *The Dynamic Meteorology of the Stratosphere and Mesosphere*, Am. Meteorol. Soc., Lancaster Press, Lancaster, Pa., 1975.

Isler, J. R., M. J. Taylor, and D. C. Fritts, Observational evidence of wave ducting and evanescence in the mesosphere, *J. Geophys. Res., 102*, 26,301-26,313, 1997.

Jones, W. L., Ducting of internal gravity waves on a stable layer with shear, *J. Geophys. Res., 77*, 3879, 1972.

Makhlouf, U. B., R. H. Picard, and J. R. Winick, Photochemical-dynamical modeling of the measured response of airglow to gravity waves, 1, Basic model for OH airglow, *J. Geophys. Res., 100*, 11,289, 1995.

Mayr, H. G., I. Harris, F. Varosi, and F. A. Herrero, Global excitation of wave phenomena in a dissipative multiconstituent medium, 1, Transfer function of the Earth's thermosphere, *J. Geophys. Res., 89*, 10,929, 1984.

Munasinghe, G., H. Hur, T. Y. Huang, A. Bhattachryya, and T. F. Tuan, Application of the dispersion formula to long- and short-period gravity waves: Comparisons with ALOHA-93 data and an analytical model, *J. Geophys. Res., 103*, 6467, 1998.

Pitteway, M. L. V., and C. O. Hines, The reflection and ducting of

atmospheric acoustic-gravity waves, *Can. J. Phys., 43*, 2222, 1965.

Reddy, C. A., Ducting of internal gravity waves in a temperature and wind stratified atmosphere, in *Internal Gravity and Acoustic Waves - A Colloquium, NCAR Tech. Note 43*, 229 pp., Natl. Cent. Atmos. Res., Boulder Colo., 1969.

Richmond, A. D., The nature of gravity wave ducting in the thermosphere, *J. Geophys. Res., 83*, 1385, 1978.

Schubert, G., and R. L. Walterscheid, Wave-driven fluctuations in OH nightglow from an extended source region, *J. Geophys. Res., 93*, 9903, 1988.

Schubert, G., R. L. Walterscheid, and M. P. Hickey, Gravity wave-driven fluctuations in OH nightglow from an extended, dissipative emission region, *J. Geophys. Res., 96*, 13,869, 1991.

Schubert, G., R. L. Walterscheid, M. P. Hickey, and C. A. Tepley, Theory and observations of gravity wave induced fluctuations in the OI (557.7 nm) airglow, *J. Geophys. Res., 104*, 14,915-14,924, 1999.

Strobel, D. F., Constraints on gravity wave induced diffusion in the middle atmosphere, *Pure Appl. Geophys., 130*, 533, 1989.

Swenson, G. R., and C. S. Gardner, Analytic models for the responses of the mesospheric OH^* and Na layers to atmospheric gravity waves, *J. Geophys. Res., 103*, 6271, 1998.

Taylor, M. J., and M. A. Hapgood, On the origin of ripple-type wave structure in the OH nightglow emission, *Planet. Space Sci., 38*, 1421, 1990.

Taylor, M. J., M. A. Hapgood, and P. Rothwell, Observations of gravity wave propagation in the OI (557.7 nm), Na (589.2 nm) and the nera infrared OH nightglow emission, *Planet. Space Sci., 35*, 413, 1987.

Taylor, M. J., M. B. Bishop, and V. Taylor, All-sky measurements of short period waves imaged in the OI (557.7 nm), Na (589.2 nm) and near infrared OH and $O_2(0,1)$ nightglow emissions during the ALOHA-93 campaign, *Geophys. Res. Lett., 22*, 2833, 1995.

Thome, G., Long period waves generated in the polar ionosphere during the onset of magnetic storms, *J. Geophys. Res., 73*, 6319, 1968.

Tuan, T-F, and D. Tadic, A dispersion formula for analyzing "model interference" among guided and free gravity wave modes and other phenomena in a realistic atmosphere, *J. Geophys. Res., 87*, 1648, 1982.

Walterscheid, R. L., G. Schubert, and J. M. Straus, A dynamical-chemical model of wave-driven fluctuations in the OH nightglow, *J. Geophys. Res., 92*, 1241, 1987.

Walterscheid, R. L., J. H. Hecht, R. Vincent, I. M. Reid, J. Woithe, and M. P. Hickey, Analysis and interpretation of airglow and radar observations of quasi-monochromatic gravity waves in the upper mesosphere and lower thermosphere over Adelaide, Australia (35° S, 138° E), *J. Atmos. Sol. Terr. Phys., 61*, 461-478, 1999.

Walterscheid, R. L., J. H. Hecht, F. T. Djuth, and C. A. Tepley, Evidence of reflection of a long-period gravity wave in observations of the nightglow over Arecibo on May 8-9, 1989, *J. Geophys. Res., 105*, 6927, 2000.

Wang, D. Y., and T.-F. Tuan, Brunt-Doppler ducting of small-period gravity waves, *J. Geophys. Res., 93*, 9916, 1988.

Wickersham, The origin and propagation of acoustic-gravity waves ducted in the thermosphere, *Aust. J. Phys., 21*, 671, 1968.

Zhang, S., R. N. Peterson, R. H. Wiens, and G. G. Shepherd, Gravity waves from O_2 nightglow during the AIDA '89 Campaign, I, Emission rate/temperature observations, *J. Atmos. Sol. Terr. Phys., 54*, 355,1993a.

Zhang, S., R. H. Wiens, and G. G. Shepherd, Gravity waves from O2 nightglow during the AIDA '89 Campaign,II, Numerical modeling of the emission rate/temperature ratio, η, *J. Atmos. Sol. Terr. Phys., 54*, 377, 1993b.

M. P. Hickey, Department of Physics and Astronomy, 308 Kinard Laboratory, Clemson University, Clemson, SC 29634-0978. (hickey@hubcap.clemson.edu)

(Received September 13, 2000; revised February 7, 2001; accepted February 20, 2001.)